Optimized Waveform Relaxation Methods for the Longitudinal Partitioning of Transmission Lines

Martin J. Gander, Mohammad Al-Khaleel and Albert E. Ruehli, *Life Fellow, IEEE*

***Abstract*—Waveform relaxation (WR) is a technique which can be used to solve large systems of ordinary differential equations (ODEs). It is especially suitable for the parallel solution of ODEs with multiple time scales, and has been successfully used for solution of electronic circuits and for solving partial differential equations (PDEs). The main issue limiting the utility of waveform relaxation is the class of problems with strong subsystem to subsystem couplings and long analysis time intervals resulting in non-uniform, slow convergence. Here we consider transmission line circuits since they represent an important part of a Spice type circuit solver. For transmission lines, the coupling between different lines is relatively weak, and thus partitioning in the transverse direction leads to very fast WR algorithms. However, longitudinal partitioning of transmission lines is very challenging due to the strong coupling which results. In this paper we propose an approach with improved convergence properties for strongly coupled longitudinal partitioning of transmission lines and other similarly strongly coupled circuits.**

***Index Terms*—Waveform relaxation and transmission lines, longitudinal partitioning, convergence analysis, fast convergence.**

I. Introduction

Transmission lines (TL) are fundamental circuit elements for the modeling of many different structures from power applications to Spice type circuit solvers. In fact, they represent one of the fundamental circuit components necessary in a Spice solver. The continuous progress of the speed and complexity of the VLSI system and semiconductor technology has required continuous improvements in transmission line models for interconnects, *e.g.* [1], [2]. Efficient TL circuit models started with the method of characteristics work [3]. Since then, approaches improved continuously in response to the ever increasing demands due to the advances in technology. Modern transmission line models are described in [4]. We will summarize some of the recent advances as an introduction to this paper, while a good list of references of the progress in TL modeling can be found in, *e.g.* [5], [6]. Multiconductor lines are of importance today for many applications such as buses. Dielectric and conductor losses have been included in the models since the '80s, *e.g.* [7]. Since then, continuous improvements have been made toward higher accuracy and larger frequency ranges of approximation, *e.g.* [8]–[10]. Hence, the quality of the multiconductor transmission line models has improved considerably over the years.

More recently, it has become clear that the next advances in computing power are due to multi-processor machines. This leads to a new area of research toward new TL models which perform well on a large number of processors. It is clear that these algorithms must fundamentally be based on splitting or partitioning of the structures into smaller units or subsystems. As part of this effort, it was recognized that the weak coupling in the important problem of multiconductor transmission lines can be exploited to subdivide each conductor into a separate subsystem using the transverse TL partitioning approach [9]. Each conductor can be solved separately using the classical Waveform Relaxation (WR) methods which were conceived in [11], [12] to speed up circuit simulation for large circuits. In the WR approach, we break a large system into many smaller subsystems, and a waveform iteration is introduced to represent the coupling between the subsystems. WR methods have the great advantage that subsystems can be solved independently with locally adapted time steps or even different time integration methods.

Problems exist for the classical WR approach in that strongly coupled, partitioned subcircuits may lead to an excessive number of waveform iterations. This diminishes the effectiveness of the approach. Hence, it is not surprising that convergence is slow with the classical WR if we attempt to further subdivide each individual TL into length sections or parts. Early on, many researchers have attempted to use classical WR for longitudinal partitioning of TLs, *e.g.* [13], but with limited success. However, the potential for parallel processing has led to a substantial research effort on the WR approach, as is evident from the references in [14]–[16] and [17]. However, the convergence issue with the classical WR has to be resolved in order to obtain efficient solvers.

WR has also been applied to the solution of Partial Differential Equations (PDEs), where coupling between subsystems which we call *transmission conditions* correspond to coupling between subdomains in physical space.

Manuscript received March 2008

M. Gander is with the *Section of Mathematics, University of Geneva,* CP 64, 1211 Geneva 4, Switzerland Mohammad Al-Khaleel, Dept. of Mathematics and Statistics, McGill University, Montreal, QC, H3A 2K6, Canada A. E. Ruehli is with T. J. Watson Research Center, IBM Research Division, Yorktown Heights, NY 10598, e-mail: ruehli@us.ibm.com

The classical WR algorithm corresponds to Dirichlet transmission conditions at the artificial interfaces between subdomains [18], [19]. However, much more effective transmission conditions can be obtained if more appropriate information, adapted to the physics of the underlying problem, is exchanged in the transmission conditions, [20]–[23]. In the circuit domain, different overlap type circuit techniques were used by several researchers to attempt convergence improvements for WR. References to early work on circuit simulations can be found in [15]. Essentially, convergence is excellent if a large portion of the tightly coupled circuit components are collected within subsystems and the coupling between subsystems is weak. Later work in [24], [25] attempted to improve coupling between subsystems to enhance the convergence of WR based methods. However, none of these techniques do include the optimization step which was introduced in the above optimized PDE work. This is also an essential step in all of our strongly coupled circuit domain work. The first approach with the optimized transmission conditions in the circuit domain was presented for diffusive (RC) circuits in [26]. It was shown that new improved coupling between subsystems can greatly enhance the performance of WR methods. More uniform convergence of the optimized WR is also of importance for strongly coupled subsystems for parallel processing, so that larger time intervals can be analyzed before exchanging waveforms between the subsystems. This reduces the communication time needed to exchange waveforms between the subsystems for parallel processing.

In this paper, we give a new formulation, which represents a generalization of the optimized WR approach which is effective for strong couplings. Specifically, we apply the technique to the very strongly coupled longitudinal transmission line partitioning problem. This optimized WR adds more flexibility and efficiency to the general WR based circuit solution for transmission line problems. *Cutting the TL wires* in the longitudinal partitioning approach represents a very challenging situation. Importantly, new work on the longitudinal circuit partitioning of transmission lines has recently shown much promise [27], [28], [29]. Also, our work lays the foundation for a general multiconductor waveform relaxation solution in the time domain. While we consider only a single line in this basic work, it is straightforward to adapt the now proved transverse WR approach in [9] to multiple lines. Our quasi-TEM section model is simple in order to be suitable for the extensive analysis required. Also, our low-loss test model is more challenging from a convergence point of view than a model which includes all the loss mechanisms.

In the next section, we derive a generalized version of the optimized WR formulation for circuits. We show mathematically that optimal transmission conditions are resulting in excellent performance for a class of circuits with strong couplings. In section III, we analyze in detail the difficult case of TEM mode type transmission line problems with longitudinal partitioning, and we derive explicit formulas for the optimized transmission conditions. Finally, in section IV, we illustrate our approach with numerical experiments.

II. Classical and Optimal Waveform Relaxation

In this section, we consider the general case of banded systems or ladder type circuits in view of the transmission line circuit problem which we want to solve. The linear circuit equations are specified as modified nodal analysis equations (MNA) in the general form

$$\mathcal{C}\dot{\boldsymbol{x}}(t) + \mathcal{G}\boldsymbol{x}(t) = \mathcal{B}\boldsymbol{u}(t), \tag{II.1}$$

where $\mathcal{C}$ contains the reactive elements and $\mathcal{G}$ the other elements, while $\mathcal{B}$ is the input selector matrix and $\boldsymbol{u}(t)$ are the forcing functions. For the systems we consider, $\mathcal{C}$ is a block diagonal, invertible matrix,

$$\mathcal{C} = \begin{bmatrix} \mathcal{C}_{1,1} & & & \\ & \mathcal{C}_{2,2} & & \\ & & \ddots & \\ & & & \mathcal{C}_{N,N} \end{bmatrix}, \tag{II.2}$$

and $\mathcal{G}$ is block tridiagonal,

$$\mathcal{G} = \begin{bmatrix} \mathcal{G}_{1,1} & \mathcal{G}_{1,2} & & \\ \mathcal{G}_{2,1} & \mathcal{G}_{2,2} & \ddots & \\ & \ddots & \ddots & \mathcal{G}_{N-1,N} \\ & & \mathcal{G}_{N,N-1} & \mathcal{G}_{N,N} \end{bmatrix}, \tag{II.3}$$

and we use $\tilde{\boldsymbol{u}}(t) := \mathcal{B}\boldsymbol{u}(t)$ to simplify the notation. The block structure suggests a natural partitioning of the system into subsystems. We denote by $\boldsymbol{s}_i$ the indices corresponding to the i-th subsystem block and we let $\mathcal{G}_{1,0} = \mathcal{G}_{N,N+1} = 0$ to avoid writing the boundary cases separately. Taking a row system at the time we obtain for i=1,2,...,N the partitions

$$\begin{aligned} \mathcal{C}_{i,i}\dot{\boldsymbol{x}}(\boldsymbol{s}_i) + \mathcal{G}_{i,i-1}\boldsymbol{x}(\boldsymbol{s}_{i-1}) + \mathcal{G}_{i,i}\boldsymbol{x}(\boldsymbol{s}_i) \\ + \mathcal{G}_{i,i+1}\boldsymbol{x}(\boldsymbol{s}_{i+1}) = \tilde{\boldsymbol{u}}_i(\boldsymbol{s}_i) \end{aligned} \tag{II.4}$$

where we denote by $\boldsymbol{x}(\boldsymbol{s}_i)$ the part of the vector $\boldsymbol{x}$ corresponding to the i-th block. For a classical waveform relaxation algorithm, we would choose the subsystem unknowns to be $\boldsymbol{x}_i$ for $i = 1, 2, \ldots, N$, and then solve iteratively for $k = 1, 2, \ldots$

$$\begin{aligned} \mathcal{C}_{i,i}\dot{\boldsymbol{x}}_i^k(\boldsymbol{s}_i) + \mathcal{G}_{i,i-1}\boldsymbol{x}_i^k(\boldsymbol{s}_{i-1}) + \mathcal{G}_{i,i}\boldsymbol{x}_i^k(\boldsymbol{s}_i) \\ + \mathcal{G}_{i,i+1}\boldsymbol{x}_i^k(\boldsymbol{s}_{i+1}) = \tilde{\boldsymbol{u}}_i(\boldsymbol{s}_i), \end{aligned} \tag{II.5}$$

together with the classical transmission conditions

$$\begin{aligned} \boldsymbol{x}_i^k(\boldsymbol{s}_{i-1}) &= \boldsymbol{x}_{i-1}^{k-1}(\boldsymbol{s}_{i-1}),\ i = 2, 3, \ldots, N, \\ \boldsymbol{x}_i^k(\boldsymbol{s}_{i+1}) &= \boldsymbol{x}_{i+1}^{k-1}(\boldsymbol{s}_{i+1}),\ i = 1, 2, \ldots, N-1, \end{aligned} \tag{II.6}$$

in order to couple the subsystems.

In the optimized WR approach, we use new transmission conditions between the subsystems which contain optimization parameters. Specifically, in the general formulation, we use the optimization operators A_i and B_i and propose on the left for $i = 2, 3, \ldots, N$ as transmission conditions

$$\begin{aligned}\mathcal{C}_{i-1,i-1}\boldsymbol{x}_i^k(\boldsymbol{s}_{i-1}) + B_{i-1}\mathcal{G}_{i-1,i}\boldsymbol{x}_i^k(\boldsymbol{s}_i) = \\ \mathcal{C}_{i-1,i-1}\boldsymbol{x}_{i-1}^{k-1}(\boldsymbol{s}_{i-1}) + B_{i-1}\mathcal{G}_{i-1,i}\boldsymbol{x}_{i-1}^{k-1}(\boldsymbol{s}_i),\end{aligned} \tag{II.7}$$

and on the right for $i = 1, 2, \ldots, N-1$ as transmission conditions

$$\begin{aligned}\mathcal{C}_{i+1,i+1}\boldsymbol{x}_i^k(\boldsymbol{s}_{i+1}) + A_i\mathcal{G}_{i+1,i}\boldsymbol{x}_i^k(\boldsymbol{s}_i) = \\ \mathcal{C}_{i+1,i+1}\boldsymbol{x}_{i+1}^{k-1}(\boldsymbol{s}_{i+1}) + A_i\mathcal{G}_{i+1,i}\boldsymbol{x}_{i+1}^{k-1}(\boldsymbol{s}_i).\end{aligned} \tag{II.8}$$

The matrix valued linear operators A_i and B_i can be chosen for this new family of waveform relaxation methods to improve the performance of the method. We first show that an optimal choice exists, with which the waveform relaxation algorithm for N subsystems converges in N iterations. To do so, we work in the frequency domain with Laplace transform parameter s. The waveform iteration is performed with a basic schedule for analyzing the N subsystems one by one. By linearity, it suffices to analyze the homogeneous case, and prove convergence to zero. Hence, we study the homogeneous Laplace transformed equation corresponding to the WR iteration in (II.5), namely for $i = 1, 2, \ldots, N$

$$\begin{aligned}\mathcal{C}_{i,i}s\hat{\boldsymbol{x}}_i^k(\boldsymbol{s}_i) + \mathcal{G}_{i,i-1}\hat{\boldsymbol{x}}_i^k(\boldsymbol{s}_{i-1}) + \mathcal{G}_{i,i}\hat{\boldsymbol{x}}_i^k(\boldsymbol{s}_i) \\ + \mathcal{G}_{i,i+1}\hat{\boldsymbol{x}}_i^k(\boldsymbol{s}_{i+1}) = \boldsymbol{0},\end{aligned} \tag{II.9}$$

and we use the new transmission conditions (II.7,II.8), which are also Laplace transformed.

Theorem 2.1 (Optimal Transmission Conditions): The waveform relaxation algorithm (II.5) with the new transmission conditions (II.7,II.8) converges in N iterations, if the Laplace symbols $\beta_i(s)$ of B_i are given by

$$\begin{aligned}\beta_1(s) &= \mathcal{C}_{1,1}(s\mathcal{C}_{1,1} + \mathcal{G}_{1,1})^{-1}, \\ \beta_i(s) &= \mathcal{C}_{i,i}(s\mathcal{C}_{i,i} + \mathcal{G}_{i,i} - \mathcal{G}_{i,i-1}\mathcal{C}_{i-1,i-1}^{-1}\beta_{i-1}(s)\mathcal{G}_{i-1,i})^{-1},\end{aligned} \tag{II.10}$$

for n=2,3,...,N-1, and the Laplace symbols $\alpha_i(s)$ of A_i are given by

$$\begin{aligned}\alpha_{N-1}(s) &= \mathcal{C}_{N,N}(s\mathcal{C}_{N,N} + \mathcal{G}_{N,N})^{-1}, \\ \alpha_{i-1}(s) &= \mathcal{C}_{i,i}(s\mathcal{C}_{i,i} + \mathcal{G}_{i,i} - \mathcal{G}_{i,i+1}\mathcal{C}_{i+1,i+1}^{-1}\alpha_i(s)\mathcal{G}_{i+1,i})^{-1},\end{aligned} \tag{II.11}$$

for $n = N-1, N-2, \ldots, 2$. independently of the initial waveforms, assuming that the matrices are invertible for all s with $\Re(s) > 0$.

Proof: The idea of the proof is to show that with the optimal choice (II.10,II.11) of transmission operators, at each iteration one additional transmission condition from the left and the right becomes homogeneous. Thus after N iterations, all subsystems have homogeneous transmission conditions. Hence, they have the zero solution.

For the first iteration, we have for the first subsystem

$$(s\mathcal{C}_{1,1} + \mathcal{G}_{1,1})\hat{\boldsymbol{x}}_1^1(\boldsymbol{s}_1) + \mathcal{G}_{1,2}\hat{\boldsymbol{x}}_1^1(\boldsymbol{s}_2) = \boldsymbol{0}. \tag{II.12}$$

Hence, if we want that the second system has a zero condition on the left in the second iteration, we need from (II.7,II.8) that $\mathcal{C}_{1,1}\hat{\boldsymbol{x}}_1^1(\boldsymbol{s}_1) + \beta_1(s)\mathcal{G}_{1,2}\hat{\boldsymbol{x}}_1^1(\boldsymbol{s}_2) = 0$, which we obtain, using that (II.12) holds, by requiring that $\mathcal{C}_{1,1} - \beta_1(s)(s\mathcal{C}_{1,1} + \mathcal{G}_{1,1}) = 0$, which leads to $\beta_1(s)$ in (II.10,II.11). With this choice of $\beta_1(s)$, for all subsequent iterations, the second subsystem has a zero condition on the left, and thus its equation, $(s\mathcal{C}_{2,2} + \mathcal{G}_{2,2})\hat{\boldsymbol{x}}_2^2(\boldsymbol{s}_2) + \mathcal{G}_{2,1}\hat{\boldsymbol{x}}_2^2(\boldsymbol{s}_1) + \mathcal{G}_{2,3}\hat{\boldsymbol{x}}_2^2(\boldsymbol{s}_3) = \boldsymbol{0}$, can be simplified to

$$(s\mathcal{C}_{2,2} + \mathcal{G}_{2,2} - \mathcal{G}_{2,1}\mathcal{C}_{1,1}^{-1}\mathcal{G}_{1,2})\hat{\boldsymbol{x}}_2^2(\boldsymbol{s}_2) + \mathcal{G}_{2,3}\hat{\boldsymbol{x}}_2^2(\boldsymbol{s}_3) = \boldsymbol{0}. \tag{II.13}$$

Now, for the third subsystem to have a zero transmission condition on the left at the third iteration, we need from (II.7,II.8) that $\mathcal{C}_{2,2}\hat{\boldsymbol{x}}_2^2(\boldsymbol{s}_2) + \beta_2(s)\mathcal{G}_{2,3}\hat{\boldsymbol{x}}_2^2(\boldsymbol{s}_3) = 0$, and since from iteration 2 on, we have (II.13), we obtain this by requiring that $\mathcal{C}_{2,2} - \beta_2(s)(s\mathcal{C}_{2,2} + \mathcal{G}_{2,2} - \mathcal{G}_{2,1}\mathcal{C}_{1,1}^{-1}\beta_1(s)\mathcal{G}_{1,2}) = 0$ which gives $\beta_2(s)$ in (II.10,II.11). With this choice, the third, and all subsequent approximations for the third subsystem satisfy the simplified equation

$$(s\mathcal{C}_{3,3} + \mathcal{G}_{3,3} - \mathcal{G}_{3,2}\mathcal{C}_{2,2}^{-1}\mathcal{G}_{2,3})\hat{\boldsymbol{x}}_3^3(\boldsymbol{s}_3) + \mathcal{G}_{3,4}\hat{\boldsymbol{x}}_3^3(\boldsymbol{s}_4) = \boldsymbol{0}. \tag{II.14}$$

By induction, we obtain now all the $\beta_i(s)$ in (II.10,II.11). A similar argument, starting with the last subsystem, leads to the results for α_i in (II.10,II.11). ■

This convergence result is optimal, since the solution of the last subsystem depends on the source terms in the first subsystem and vice versa, and because information is only communicated locally to neighboring subsystems in each iteration. In general, convergence of the algorithm in less than N steps is not possible.

The proof of Theorem 2.1 also suggest a different subsystem scheduling sequence: instead of solving all subsystems at each iteration, and then exchanging information between subsystems, one could just solve the first and last one in the first iteration, and then the second and second last in the second iteration, and so on. The method would still converge in N iterations, and at each iteration step only two subsystems would need to be solved. However, other schedules may be more desirable once the location of the sources is known, or have more parallelism.

The symbols $\alpha_i(s)$ and $\beta_i(s)$ in (II.10,II.11) are matrices whose entries are not polynomials in s. Hence, they correspond to convolution operators in time at the interfaces between subsystems, which are much more costly than the classical transmission conditions (II.6). For this reason, we investigate approximations to the optimal transmission conditions. In section III-C, we give an example of how such an approximation can be optimized for transmission line problems.

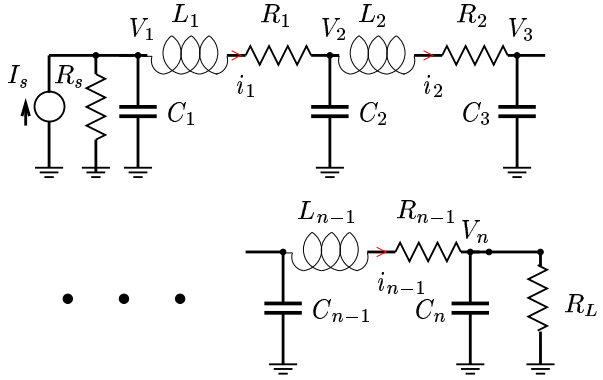

Fig. 1. A transmission line with transport behavior.

III. The Transmission Line Problem

In this section, we apply the new waveform relaxation algorithm from the previous section to the TEM mode type transmission line model shown in Figure 1. The MNA circuit matrices (II.1) for the TEM model are

$$\mathcal{C} = \begin{bmatrix} C_1 & & & & & & \\ & L_1 & & & & & \\ & & C_2 & & & & \\ & & & L_2 & & & \\ & & & & \ddots & & \\ & & & & & L_{n-1} & \\ & & & & & & C_n \end{bmatrix},$$

$$\mathcal{G} = \begin{bmatrix} \frac{1}{R_s} & 1 & & & & & \\ -1 & R_1 & 1 & & & & \\ & -1 & 0 & 1 & & & \\ & & -1 & R_2 & 1 & & \\ & & & \ddots & \ddots & \ddots & \\ & & & & -1 & R_{n-1} & 1 \\ & & & & & -1 & \frac{1}{R_L} \end{bmatrix}. \quad \text{(III.1)}$$

For the tridiagonal structure of the ladder circuit considered, the matrices $\mathcal{G}_{i,j}$, $j = i \pm 1$ only contain one non-zero entry, which simplifies both the classical and new transmission conditions in the general waveform relaxation algorithm (II.5): only a scalar value needs to be transmitted. Denoting by $\boldsymbol{s}_i^f$ the first and $\boldsymbol{s}_i^l$ the last entry in the index set $\boldsymbol{s}_i$, the classical transmission conditions are

$$\begin{aligned} \boldsymbol{x}_i^k(\boldsymbol{s}_{i-1}^l) &= \boldsymbol{x}_{i-1}^{k-1}(\boldsymbol{s}_{i-1}^l),\ i = 2,3,\ldots,N, \\ \boldsymbol{x}_i^k(\boldsymbol{s}_{i+1}^f) &= \boldsymbol{x}_{i+1}^{k-1}(\boldsymbol{s}_{i+1}^f),\ i = 1,2,\ldots,N-1, \end{aligned} \quad \text{(III.2)}$$

which now exchange only a scalar value at the interfaces. Similarly, the new transmission conditions are on the left for $i = 2,3,\ldots,N$

$$\boldsymbol{x}_i^k(\boldsymbol{s}_{i-1}^l) + B_{i-1}\boldsymbol{x}_i^k(\boldsymbol{s}_i^f) = \boldsymbol{x}_{i-1}^{k-1}(\boldsymbol{s}_{i-1}^l) + B_{i-1}\boldsymbol{x}_{i-1}^{k-1}(\boldsymbol{s}_i^f), \quad \text{(III.3)}$$

and on the right for $i = 1,2,\ldots,N-1$

$$\boldsymbol{x}_i^k(\boldsymbol{s}_{i+1}^f) + A_i\boldsymbol{x}_i^k(\boldsymbol{s}_i^l) = \boldsymbol{x}_{i+1}^{k-1}(\boldsymbol{s}_{i+1}^f) + A_i\boldsymbol{x}_{i+1}^{k-1}(\boldsymbol{s}_i^l), \quad \text{(III.4)}$$

where A_i and B_i are reduced to scalar linear operators. Theorem 2.1 gives the optimal choice of these non-local convolution operators. To make the approach applicable to real-life problems, we want to find local approximations where A_i and B_i are as simple as possible. This leads to an algorithm which is as straightforward to implement as the classical WR algorithm. Importantly, for a good choice of A_i and B_i, fast convergence can be achieved for problems where the application of the classical WR algorithm is inefficient. Considerable research work has been devoted to determine a good choice of the local approximations. For example, in [28] we presented a study for a small transmission line circuit consisting of two sections only. Here, we extensively study the case of an infinitely long transmission line. The equations of the infinitely long circuit are of the form

$$\dot{\boldsymbol{x}} = \begin{bmatrix} \ddots & \ddots & \ddots & & & & \\ & a & b & -a & & & \\ & & -c & 0 & c & & \\ & & & a & b & -a & \\ & & & & -c & 0 & c \\ & & & & & \ddots & \ddots & \ddots \end{bmatrix} \boldsymbol{x} + \boldsymbol{f}, \quad \text{(III.5)}$$

where $\boldsymbol{x} = (\ldots, x(-2), x(-1), x(0), x(1), x(2), \ldots)^T$, and the entries of the matrix after multiplication by the inverse of the matrix $\mathcal{C}$ are given by

$$a = \frac{1}{L}, \quad c = -\frac{1}{C}, \quad b = -\frac{R}{L}. \quad \text{(III.6)}$$

Since the circuit is infinitely large, we assume that all voltage and current values stay bounded as we approach the infinite ends of the circuit in the analysis in order to have a well posed problem.

A. Analysis for Classical WR Algorithms

From the MNA circuit equations (III.1) it is evident that taking the even or odd rows switches between current and voltage unknowns. Hence, the type of partitioning alternates. However, if an overlap is used, both types of variables will be covered. We first partition the circuit corresponding to an infinitely long line at an even row into two sub-circuits or subsystems without overlapping unknowns. We call the unknown values in the first subsystem $\boldsymbol{x}_1(t)$ and in the second subsystem $\boldsymbol{x}_2(t)$, which

leads to the classical WR algorithm

$$\dot{\boldsymbol{x}}_1^k = \begin{bmatrix} \ddots & \ddots & \ddots & \\ & -c & 0 & c \\ & & a & b \end{bmatrix} \boldsymbol{x}_1^k + \begin{pmatrix} \vdots \\ f(-1) \\ f(0) \end{pmatrix} + \begin{pmatrix} \vdots \\ 0 \\ -a\boldsymbol{x}_2^{k-1}(1) \end{pmatrix},$$
$$\dot{\boldsymbol{x}}_2^k = \begin{bmatrix} 0 & c & & \\ a & b & -a & \\ & \ddots & \ddots & \ddots \end{bmatrix} \boldsymbol{x}_2^k + \begin{pmatrix} f(1) \\ f(2) \\ \vdots \end{pmatrix} + \begin{pmatrix} -c\boldsymbol{x}_1^{k-1}(0) \\ 0 \\ \vdots \end{pmatrix}. \tag{III.7}$$

For the infinite system the rows with 0 diagonal elements with c off diagonal elements correspond to voltage unknowns while the alternative rows with a and b elements correspond to current unknowns. As done in section II, we analyze the convergence for the homogeneous problem, $\boldsymbol{f}(t) = \boldsymbol{0}$, with zero initial conditions $\boldsymbol{x}(0) = \boldsymbol{0}$ for the convergence study.

The Laplace transform with $s \in \mathbb{C}$ of the homogeneous classical WR problem yields

$$s\hat{\boldsymbol{x}}_1^k = \begin{bmatrix} \ddots & \ddots & \ddots & \\ & -c & 0 & c \\ & & a & b \end{bmatrix} \hat{\boldsymbol{x}}_1^k + \begin{pmatrix} \vdots \\ 0 \\ -a\hat{\boldsymbol{x}}_2^{k-1}(1) \end{pmatrix},$$
$$s\hat{\boldsymbol{x}}_2^k = \begin{bmatrix} 0 & c & & \\ a & b & -a & \\ & \ddots & \ddots & \ddots \end{bmatrix} \hat{\boldsymbol{x}}_2^k + \begin{pmatrix} -c\hat{\boldsymbol{x}}_1^{k-1}(0) \\ 0 \\ \vdots \end{pmatrix}. \tag{III.8}$$

Solving the first system of equations for $\hat{\boldsymbol{x}}_1^k(j)$ corresponds to solving the recurrence relations

$$\begin{aligned} a\hat{\boldsymbol{x}}_1^k(j-1)+(b-s)\hat{\boldsymbol{x}}_1^k(j)-a\hat{\boldsymbol{x}}_1^k(j+1)=0, j=0,-2\ldots, \\ -c\hat{\boldsymbol{x}}_1^k(j-1)-s\hat{\boldsymbol{x}}_1^k(j)+c\hat{\boldsymbol{x}}_1^k(j+1)=0, j=-1,-3\ldots, \end{aligned}$$

in j, or equivalently for $j = 0, -1, -2, \ldots$

$$\begin{aligned} a\hat{\boldsymbol{x}}_1^k(2j-1) + (b-s)\hat{\boldsymbol{x}}_1^k(2j) - a\hat{\boldsymbol{x}}_1^k(2j+1) &= 0, \\ -c\hat{\boldsymbol{x}}_1^k(2j-2) - s\hat{\boldsymbol{x}}_1^k(2j-1) + c\hat{\boldsymbol{x}}_1^k(2j) &= 0. \end{aligned} \tag{III.9}$$

Solving the second equation in (III.9) for the odd indices, with $s = \eta + i\omega$, $\eta > 0$, we get $\hat{\boldsymbol{x}}_1^k(2j-1) = \frac{c}{s}(\hat{\boldsymbol{x}}_1^k(2j) - \hat{\boldsymbol{x}}_1^k(2j-2))$, and substituting this result into the other equation, we find for $j = 0, -1, -2, \ldots$ the recurrence relation

$$-\frac{ac}{s}\hat{\boldsymbol{x}}_1^k(2j-2)+(\frac{2ac}{s}+(b-s))\hat{\boldsymbol{x}}_1^k(2j)-\frac{ac}{s}\hat{\boldsymbol{x}}_1^k(2j+2)=0, \tag{III.10}$$

Since all circuit elements are positive, we have $a > 0$, $b < 0$, and $c < 0$ from (III.6), and we obtain for $j = 0, -1, -2, \ldots$

$$\frac{a|c|}{s}\hat{\boldsymbol{x}}_1^k(2j-2)-(\frac{2a|c|}{s}+(|b|+s))\hat{\boldsymbol{x}}_1^k(2j)+\frac{a|c|}{s}\hat{\boldsymbol{x}}_1^k(2j+2)=0. \tag{III.11}$$

The general solution of (III.11) is therefore

$$\hat{\boldsymbol{x}}_1^k(2j) = A^k\lambda_+^{2j} + B^k\lambda_-^{2j}, \tag{III.12}$$

where $\lambda_\pm^2$ are the roots of the characteristic polynomial of the recurrence relation,

$$\lambda_\pm^2 = \frac{2a|c|+s(|b|+s)\pm\sqrt{(2a|c|+s(|b|+s))^2-4a^2|c|^2}}{2a|c|}, \tag{III.13}$$

and A^k, B^k are some constants.

Lemma 3.1: The roots $\lambda_\pm^2$ given in equation (III.13) satisfy for $s = \eta + i\omega$, $\eta \geq 0$,

- $|\lambda_+^2| > 1$ for $\{(\eta,\omega) : -\sqrt{2a|c| + |b|\eta + \eta^2} < \omega \leq \sqrt{2a|c| + |b|\eta + \eta^2},\ \eta \geq 0\} \setminus \{(0,0)\}$,
- $|\lambda_-^2| > 1$ for $\{(\eta,\omega) : \omega \leq -\sqrt{2a|c| + |b|\eta + \eta^2}$, or $\omega > \sqrt{2a|c| + |b|\eta + \eta^2},\ \eta \geq 0\}$,
- $|\lambda_+^2| = |\lambda_-^2| = 1 \iff \lambda_+^2 = \lambda_-^2 = 1 \iff \omega = \eta = 0$.

Proof: The proof of this results is technical and can be found in [29]. ■

To determine the constants A^k and B^k for the general solution (III.12), we need to use the transmission conditions at the subsystem interfaces and the boundedness condition at infinity. We first consider the case when $|\lambda_+^2| > 1$, which implies $|\lambda_-^2| < 1$, since $|\lambda_+^2||\lambda_-^2| = 1$, and thus by the boundedness assumption on the solution, we obtain $B^k = 0$. Hence, $\hat{\boldsymbol{x}}_1^k(2j) = A^k\lambda_+^{2j}$ and $\hat{\boldsymbol{x}}_1^k(2j-1) = \frac{c}{s}A^k\lambda_+^{2j-2}(\lambda_+^2 - 1)$. To determine A^k, we use the last equation of the first subsystem at the interface

$$a\hat{\boldsymbol{x}}_1^k(-1)+(b-s)\hat{\boldsymbol{x}}_1^k(0)=A^k(\frac{ac}{s}(1-\lambda_+^{-2})+b-s)=a\hat{\boldsymbol{x}}_2^{k-1}(1),$$

which leads to $A^k = \frac{as\hat{\boldsymbol{x}}_2^{k-1}(1)}{ac(1-\lambda_+^{-2})+s(b-s)}$, and by Vieta's formulas we have $\lambda_+^2 + \lambda_-^2 = \frac{s(b-s)}{ac} + 2$, and thus we can simplify A^k to

$$A^k = \frac{s\hat{\boldsymbol{x}}_2^{k-1}(1)}{c(\lambda_+^2 - 1)}.$$

Hence the general solutions for $\hat{\boldsymbol{x}}_1^k(2j)$ and $\hat{\boldsymbol{x}}_1^k(2j-1)$, $j = 0, -1, -2, \ldots$, are given by

$$\hat{\boldsymbol{x}}_1^k(2j) = \frac{s\hat{\boldsymbol{x}}_2^{k-1}(1)}{c(\lambda_+^2 - 1)}\lambda_+^{2j}, \quad \hat{\boldsymbol{x}}_1^k(2j-1) = \hat{\boldsymbol{x}}_2^{k-1}(1)\lambda_+^{2j-2}. \tag{III.14}$$

By a similar calculation, we obtain for the second subsystem for $j = 1, 2, 3, \ldots$ the solutions

$$\hat{\boldsymbol{x}}_2^k(2j)=\hat{\boldsymbol{x}}_1^{k-1}(0)\lambda_-^{2j}, \hat{\boldsymbol{x}}_2^k(2j-1)=\frac{c(\lambda_-^2-1)\hat{\boldsymbol{x}}_1^{k-1}(0)}{s}\lambda_-^{2j-2}. \tag{III.15}$$

Inserting this result at iteration k into (III.14), we find over two iteration steps of the WR algorithm the mapping

$$\hat{\boldsymbol{x}}_1^{k+1}(0) = \rho_{cla}(s,a,b,c)\hat{\boldsymbol{x}}_1^{k-1}(0),$$

with the convergence factor ρ_{cla} given by

$$\rho_{cla}(s,a,b,c) = \frac{\lambda_-^2 - 1}{\lambda_+^2 - 1} = -\lambda_-^2, \tag{III.16}$$

where we used $\lambda_+^2\lambda_-^2 = 1$ to obtain the last equality on the right. The second case is when $|\lambda_-^2| > 1$, and for this case, we obtain with a similar calculation

$$\rho_{cla}(s,a,b,c) = \frac{\lambda_+^2 - 1}{\lambda_-^2 - 1} = -\lambda_+^2. \qquad \text{(III.17)}$$

The case where $\lambda_\pm^2 = 1$, implies that $s = 0$, i.e. $\eta = \omega = 0$. Note that the limit of ρ_{cla} as $s \to 0$ equals 1 and the algorithm is not convergent. To summarize, we have for $\eta > 0$

$$\rho_{cla}(s,a,b,c) = \begin{cases} -\lambda_-^2, & |\lambda_+^2| > 1, \\ -\lambda_+^2, & |\lambda_+^2| < 1. \end{cases} \qquad \text{(III.18)}$$

Similar calculations show that the same convergence factor ρ_{cla} is also found if we partition the circuit at an odd row. This will be different for the new WR algorithm as we will see later. The following Theorem shows that the convergence factor (III.18) is an analytic function for $\eta > 0$, which allows us to use the maximum principle for complex analytic functions in what follows.

Theorem 3.2: If $a > 0$, $b < 0$, and $c < 0$, then the convergence factor ρ_{cla} of the classical WR in (III.18) is an analytic function of s in the right half of the complex plane.

Proof: The proof is technical and can be found in [29]. ■

We can now estimate the convergence of the classical WR algorithm applied to the transmission line problem. By the maximum principle for analytic functions, the maximum of $|\rho_{cla}(s)|$ for $s = \eta + i\omega$, $\eta > 0$ is on the boundary of the right half of the complex plane, and since for $s = re^{i\theta}$, $-\pi/2 < \theta < \pi/2$, we have $\lim_{r\to\infty} \rho_{cla} = 0$, for both cases $|\lambda_+^2| > 1$ and $|\lambda_+^2| < 1$, the maximum will be at $\eta = 0$. Unfortunately for $\eta = 0$, as ω goes to zero, we find that $|\rho_{cla}|$ goes to one, and hence convergence will be very slow for low frequencies, ω close to zero. An example for the convergence factor as a function of ω for $\eta = 0$ is given in Figure 2. This explains why longitudinal partitioning of transmission lines leads to very slow convergence in general.

If we overlap the unknowns by one, we can show using a similar analysis that the convergence factor becomes

$$\rho_{cla}(s,a,b,c) = \begin{cases} (\lambda_-^2)^2, & |\lambda_+^2| > 1, \\ (\lambda_+^2)^2, & |\lambda_+^2| < 1. \end{cases} \qquad \text{(III.19)}$$

In both cases of a cut at an even or at an odd row we have the square of the convergence factor without overlap of the unknowns. This shows that overlap improves the convergence behavior, but it can not correct the severe convergence problem of longitudinal partitioning of transmission lines, since low frequencies still converge arbitrary slowly. In the next section, we will show for the overlapping case how an optimized WR algorithm can be obtained. A similar approach could also be developed for the case without overlap.

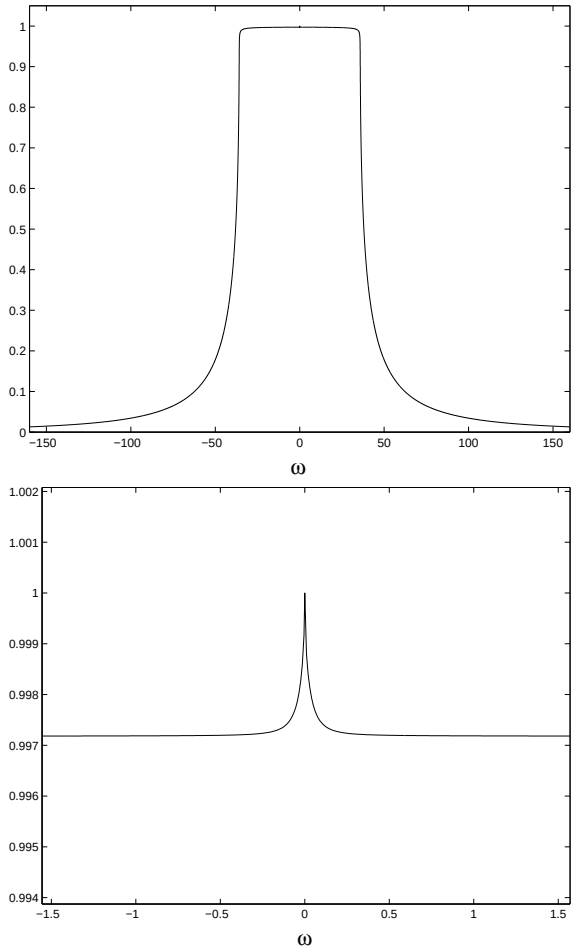

Fig. 2. Convergence factor $|\rho_{cla}(\omega)|$ for $\eta = 0$ as a function of the frequency parameter ω on the left, and zoom on the right showing $|\rho_{cla}|$ for ω around zero.

B. Analysis for Optimized WR Algorithms

With the new transmission conditions with a cut at an even row, which are

$$\begin{aligned} \boldsymbol{x}_1^k(1) + \alpha \boldsymbol{x}_1^k(0) &= \boldsymbol{x}_2^{k-1}(1) + \alpha \boldsymbol{x}_2^{k-1}(0), \\ \boldsymbol{x}_2^k(0) + \beta \boldsymbol{x}_2^k(-1) &= \boldsymbol{x}_1^{k-1}(0) + \beta \boldsymbol{x}_1^{k-1}(-1), \end{aligned} \qquad \text{(III.20)}$$

we obtain the new waveform relaxation algorithm

$$\begin{aligned} \dot{\boldsymbol{x}}_1^k &= \begin{bmatrix} \ddots & \ddots & \ddots & \\ & -c & 0 & c \\ & & a & b+a\alpha \end{bmatrix} \boldsymbol{x}_1^k + \begin{pmatrix} \vdots \\ f(-1) \\ f(0) - a(\boldsymbol{x}_2^{k-1}(1) + \alpha \boldsymbol{x}_2^{k-1}(0)) \end{pmatrix}, \\ \dot{\boldsymbol{x}}_2^k &= \begin{bmatrix} b - \frac{a}{\beta} - a & & \\ -c & 0 & c \\ & \ddots & \ddots & \ddots \end{bmatrix} \boldsymbol{x}_2^k + \begin{pmatrix} f(0) + \frac{a}{\beta}(\boldsymbol{x}_1^{k-1}(0) + \beta \boldsymbol{x}_1^{k-1}(-1)) \\ f(1) \\ \vdots \end{pmatrix}. \end{aligned} \qquad \text{(III.21)}$$

Using a similar analysis as for the classical waveform relaxation algorithm, we find that the convergence factor

of the new waveform relaxation algorithm is

$$\rho_{opt}(s,a,b,c,\alpha,\beta)=\begin{cases}\frac{c(\lambda_-^2-1)+\alpha s}{c(\lambda_+^2-1)+\alpha s}\,\frac{\beta c(1-\lambda_-^2)+s}{\beta c(1-\lambda_+^2)+s}, & |\lambda_+^2|>1,\\ \frac{c(\lambda_+^2-1)+\alpha s}{c(\lambda_-^2-1)+\alpha s}\,\frac{\beta c(1-\lambda_+^2)+s}{\beta c(1-\lambda_-^2)+s}, & |\lambda_+^2|<1.\end{cases} \tag{III.22}$$

From (III.22), we see that the optimal transmission operators would have the symbols

$$\begin{aligned}\hat{\alpha}_{even}&=-\tfrac{c(\lambda_-^2-1)}{s},\ \hat{\beta}_{even}=-\tfrac{s}{c(1-\lambda_-^2)},\ |\lambda_+^2|>1,\\ \hat{\alpha}_{even}&=-\tfrac{c(\lambda_+^2-1)}{s},\ \hat{\beta}_{even}=-\tfrac{s}{c(1-\lambda_+^2)},\ |\lambda_+^2|<1.\end{aligned} \tag{III.23}$$

If we cut at an odd row, we obtain the convergence factor

$$\rho_{opt}(s,a,b,c,\alpha,\beta)=\begin{cases}\frac{s\lambda_-^2+\alpha c(\lambda_-^2-1)}{s+\alpha c(1-\lambda_-^2)}\,\frac{c(1-\lambda_-^2)+\beta s\lambda_-^2}{c(\lambda_-^2-1)+\beta s}, & |\lambda_+^2|>1,\\ \frac{s\lambda_+^2+\alpha c(\lambda_+^2-1)}{s+\alpha c(1-\lambda_+^2)}\,\frac{c(1-\lambda_+^2)+\beta s\lambda_+^2}{c(\lambda_+^2-1)+\beta s}, & |\lambda_+^2|<1,\end{cases} \tag{III.24}$$

and the optimal transmission operator symbols are

$$\begin{aligned}\hat{\alpha}_{odd}&=-\tfrac{s}{c(1-\lambda_+^2)},\ \hat{\beta}_{odd}=\tfrac{c(1-\lambda_+^2)}{s},\ |\lambda_+^2|>1,\\ \hat{\alpha}_{odd}&=-\tfrac{s}{c(1-\lambda_-^2)},\ \hat{\beta}_{odd}=\tfrac{c(1-\lambda_-^2)}{s},\ |\lambda_+^2|<1.\end{aligned} \tag{III.25}$$

It is interesting to note that a relation exist between the optimal choices obtained with overlap at an even row and at an odd row; we have

$$\hat{\beta}_{even}=-\hat{\alpha}_{odd}-\frac{s}{c},\quad \hat{\alpha}_{even}=-\hat{\beta}_{odd}-\frac{b}{a}+\frac{s}{a}. \tag{III.26}$$

If we approximate $\hat{\alpha}_{odd}$ and $\hat{\beta}_{odd}$ by a constant, we can deduce first order transmission conditions for the cut at an even row. We therefore analyze in what follows the constant approximation of the optimal choice in (III.25) for the new WR algorithm with overlap at an odd row. The following theorem asserts again that the convergence factor ρ_{opt} is analytic in the right half of the complex plane, which allows us to use the maximum principle in the optimization.

Theorem 3.3: If $a>0$, $b<0$ and $c<0$, then the convergence factor ρ_{opt} in (III.24) is an analytic function in the right half of the complex plane, $s=\eta+i\omega$, $\eta>0$, provided that

$$\alpha<0,\quad \beta>0. \tag{III.27}$$

Proof: The proof is technical and can be found in [29]. ■

We can now estimate the convergence of the new WR algorithm applied to the transmission line problem. By the maximum principle for analytic functions, the maximum of $|\rho_{opt}(s)|$ for $s=\eta+i\omega$, $\eta>0$ is on the boundary of the right half of the complex plane. We now take $s=re^{i\theta}$, $-\pi/2<\theta<\pi/2$, to see that when $|\lambda_+^2|>1$, the limit as $r\to\infty$ is zero, and the same limit is also obtained for the case when $|\lambda_-^2|>1$. Therefore, the maximum of $|\rho_{opt}|$ in the right half of the complex plane is attained at $\eta=0$. However, similar to the classical WR algorithm, as noted earlier, taking the limit on the boundary $\eta=0$ as ω goes to zero, we find that $|\rho_{opt}|=1$, and the zero mode does not converge. However, since finite time signals are band limited, we can truncate the frequency range by a minimal frequency. This is important for our problem in the optimization process described below. This process is simplified by the following:

Lemma 3.4: The modulus of the convergence factor ρ_{opt} in (III.24), for $s=i\omega$, satisfies

$$|\rho_{opt}(i|\omega|,a,b,c,\alpha,\beta)|=|\rho_{opt}(-i|\omega|,a,b,c,\alpha,\beta)|.$$

Proof: The proof is again technical and can be found in [29]. ■

By Lemma 3.4, we can optimize for positive frequencies only, $\omega>0$, and we get the min-max problem

$$\min_{\alpha<0,\beta>0}\left(\max_{0<\omega_{min}\le\omega\le\omega_{max}}|\rho_{opt}(i\omega,a,b,c,\alpha,\beta)|\right), \tag{III.28}$$

where we band limited the frequency range by minimal and maximal, practically relevant frequencies for the problem. Simple estimates can be derived as $\omega_{min}=\frac{\pi}{T}$ and $\omega_{max}=\frac{\pi}{\Delta t}$; the lowest frequency is estimated from the maximum transient analysis time T and the highest frequency from the time step Δt.

C. Solution of the Optimization Problem

The min-max problem (III.28) cannot be solved in closed form in general, even with the simplifying assumption $\beta=-\frac{1}{\alpha}$, which is motivated by the optimal choice found in (III.23), and by the symmetry of the circuit. The dashed line in Figure 4 was obtained by numerically solving the min-max optimization problem. It shows the dependence of the optimized parameter α^* on the transient analysis time T for the typical choice of transmission line parameters per unit length

$$L=4.95\ 10^{-3}\,\frac{\mu\mathrm{H}}{\mathrm{cm}},C=0.63\,\frac{\mathrm{pF}}{\mathrm{cm}},R=0.5\ 10^{-3}\,\frac{\mathrm{kOhm}}{\mathrm{cm}}. \tag{III.29}$$

In this work T is specified in ns. For small T, the optimal choice α^* is small. This is consistent with the fast convergence of the classical WR for very small time intervals [30]. Then it grows for larger values of T, until it suddenly grows rapidly to a certain threshold which, for this example, is about $T=0.1$. The optimum then stays constant over a long range of increasing values of T, until it finally starts to decrease again slowly for further increasing values of T. In order to understand this phenomenon, we look for the three cases at the associated optimized convergence factor ρ. Figure 3 shows the case when $T=0.05$ on top, $T=5$ in the middle, and $T=10^5$ on the bottom. This confirms that convergence is very rapid for short time intervals, and slower for long time

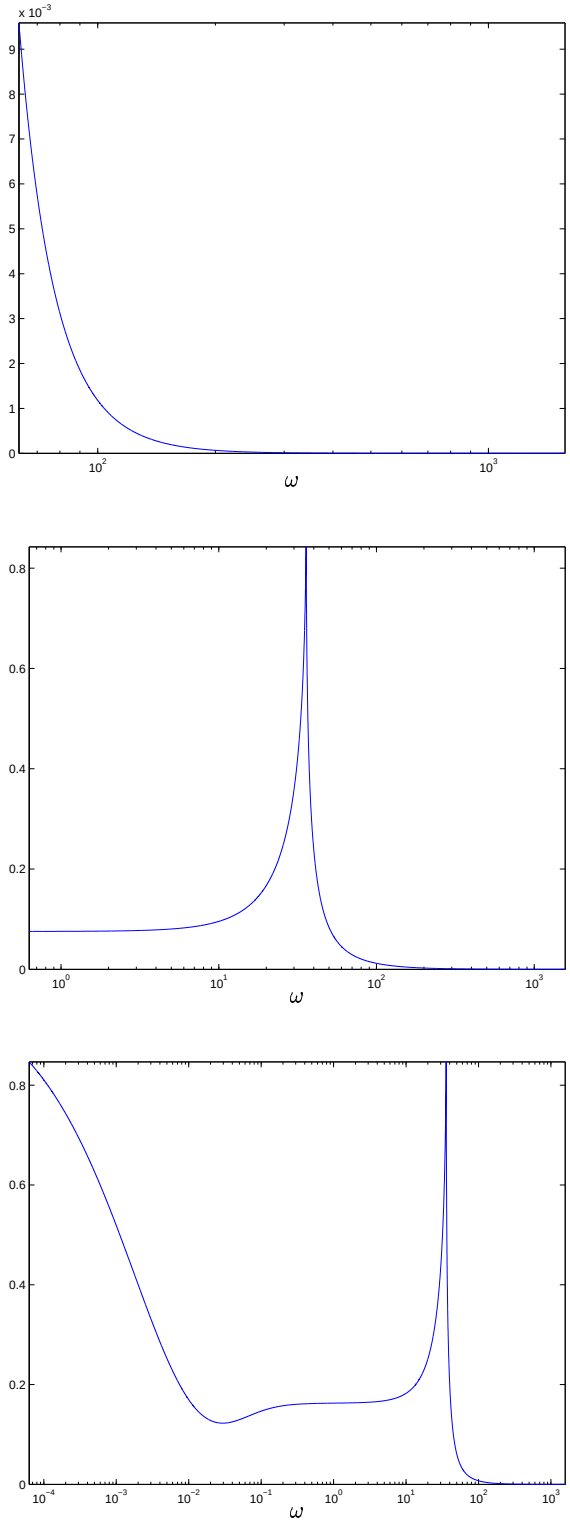

Fig. 3. Numerically optimized convergence factor $|\rho|$ for $T = 0.05$ on top, $T = 5$ in the middle, and $T = 10^5$ on the bottom.

intervals. We also observe that the optimized parameter α^* is determined for short time by a minimization for the lowest frequency in the spectrum, for intermediate time intervals by a minimization of the maximum somewhere in the middle of the relevant frequencies, and for large time intervals by equioscillation of the lowest frequency and the frequency at the maximum. This insight corresponds well to the three regimes represented by the dashed line in Fig. 4.

Of course, for practical applications we must have simple ways to find the appropriate value of the α^*. To obtain explicit formulas for α^* as a function of the transmission line parameters (III.29), we study asymptotically the min-max problem (III.28) for T small and T large. The in-between values are found below.

When T is large, our numerical experiments have shown that the solution of the min-max problem (III.28) with the choice $\beta = -\frac{1}{\alpha}$ occurs when the convergence factor at $\omega = \omega_{min}$ and at $\omega = \overline{\omega}$ are balanced, where ω_{min} is small and $\overline{\omega}$ is the interior maximum of $|\rho_{opt}|$. Therefore, α^* satisfies the equation

$$r(\omega_{min}, a, b, c, \alpha^*) = r(\overline{\omega}, a, b, c, \alpha^*), \qquad \text{(III.30)}$$

where $r(\omega, a, b, c, \alpha) := |\rho_{opt}(i\omega, a, b, c, \alpha, -\frac{1}{\alpha})|$, and ρ_{opt} is given in (III.24). With this choice of α^*, $r(\omega, a, b, c, \alpha^*) \leq r(\omega_{min}, a, b, c, \alpha^*) := \bar{r}_l$ for all $\omega \geq \omega_{min}$.

To obtain an explicit formula for the optimized parameter α^*, we use asymptotic analysis. Since we can estimate $\omega_{\min}$ by $\frac{\pi}{T}$, $\omega_{\min}$ is small for T large, so we set $\omega_{min} := \epsilon$, and solve (III.30) asymptotically for small ϵ. We use the ansatz $\alpha = C_\alpha \epsilon^{\gamma_1}$, and $\overline{\omega} = C_\omega \epsilon^{\gamma_2}$. Inserting this ansatz into the polynomial $P(\omega)$ obtained from the partial derivative of r with respect to ω, which gives the extrema of r, we obtain after a lengthy calculation the leading order terms

$$P(\overline{\omega}) = \sqrt{2abc} C_\omega^4 a^2 \epsilon^{4\gamma_2} - 2\sqrt{2abc} a^2 c C_\omega^3 C_\alpha \epsilon^{\gamma_1 + 3\gamma_2} + \dots.$$

Similarly, expanding equation (III.30) for ϵ small, we find the leading order terms

$$1 + \frac{2\sqrt{2abc}}{bcC_\alpha}\epsilon^{1/2-\gamma_1} + \dots = 1 + \frac{\sqrt{2abc}C_\alpha}{aC_\omega^{1/2}}\epsilon^{\gamma_1 - \gamma_2/2} + \frac{\sqrt{2abc}C_\omega^{1/2}}{ac}\epsilon^{\gamma_2/2} + \dots.$$

Equating the exponents in the expansions leads to $\gamma_1 = \frac{1}{3}$ and $\gamma_2 = \frac{1}{3}$, and from matching the constants in these leading order terms, we obtain

$$C_\alpha = \frac{2^{1/3}\left(\frac{a\sqrt{2}c}{b}\right)^{2/3}}{2c}, \quad C_\omega = 2^{1/3}\left(\frac{a\sqrt{2}c}{b}\right)^{2/3},$$

which leads to the explicit, asymptotically optimized formula for the optimized parameter α_l^*, where the index l

stands for 'long T',

$$\alpha_l^* = \frac{(2\pi)^{1/3}\left(\frac{\sqrt{2}ac}{b}\right)^{2/3}}{2cT^{1/3}} = -\frac{(4\pi C)^{1/3}}{2R^{2/3}T^{1/3}} \quad \text{for } T \text{ large.} \tag{III.31}$$

Using this optimized parameter, the asymptotic contraction factor of the optimized waveform relaxation algorithm becomes for T large

$$\bar{r}_l \sim 1 - \frac{2^{11/6}\pi^{1/6}(-b)^{1/6}}{a^{1/6}(-c)^{1/6}T^{1/6}} = 1 - \frac{2^{11/6}\pi^{1/6}(RC)^{1/6}}{T^{1/6}} \tag{III.32}$$

With a similar asymptotic analysis for T small, we find that one has to minimize r at $\omega_{\min}$, *i.e.* one has to solve asymptotically for T small the equation

$$\frac{\partial}{\partial\alpha} r(\omega_{\min}, a, b, c, \alpha^*) = 0, \tag{III.33}$$

which leads to the optimized formula

$$\alpha_s^* = \frac{ba}{\pi^2}T^2 = -\frac{RT^2}{\pi^2 L^2} \quad \text{for } T \text{ small,} \tag{III.34}$$

with the associated asymptotic contraction factor

$$\bar{r}_s \sim \frac{a^2c^2}{\pi^4}T^4 = \frac{1}{L^2C^2\pi^4}T^4. \tag{III.35}$$

This shows that the convergence rate is very rapid for small T, a typical feature of all waveform relaxation algorithms.

Unfortunately, the most difficult case is also the most important one in practice. It is the case for intermediate values of T, where interestingly the optimized parameter α^* seems to become independent of T, as we have observed in the dashed line in Fig. 4. In this case, as we have seen from the numerical experiments in Fig. 3, the optimized α^* is determined by minimizing the interior maximum, *i.e.* we have to solve the system of equations

$$\frac{\partial}{\partial\omega} r(\overline{\omega}, a, b, c, \alpha^*) = 0, \qquad \frac{\partial}{\partial\alpha^*} r(\overline{\omega}, a, b, c, \alpha^*) = 0 \tag{III.36}$$

for α^* and $\overline{\omega}$. In order to obtain an explicit formula, we use the fact that a transmission line can be represented by smaller and smaller sections. If we used, for example, n sections per unit length, the characteristic electronic component parameters would be

$$L_i = \frac{L}{n}\ \mu\text{H},\ C_i = \frac{C}{n}\ \text{pF},\ R_i = \frac{R}{n}\ \text{kOhms.} \tag{III.37}$$

We thus expand the system of equations (III.36) for n large, and find after a very long and technically challenging analysis the marvelously simple result

$$\alpha_m^* = \sqrt{\frac{C}{3L}} \quad \text{for intermediate } T, \tag{III.38}$$

with the associated asymptotic convergence factor

$$\bar{r}_m \sim 1 - \frac{(3+3^{1/2})C^{1/4}\sqrt{R}}{L^{1/4}\sqrt{n}}. \tag{III.39}$$

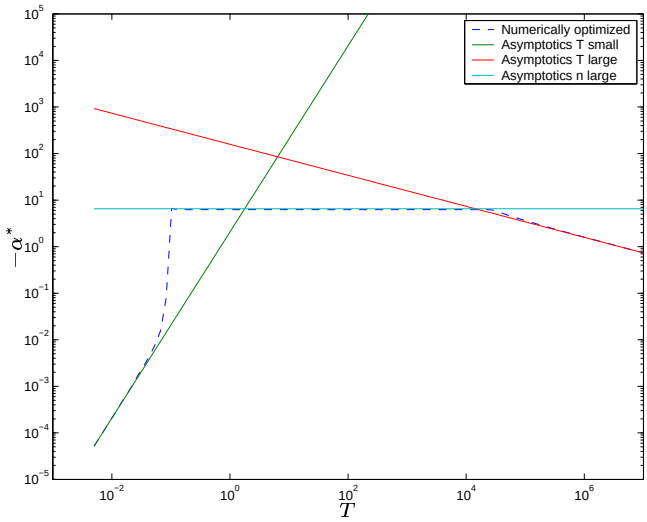

Fig. 4. Numerically optimized parameter α^* as a function of the length of the time interval for a typical transmission line, together with our asymptotically optimized explicit formulas.

We show in Fig. 4 the three asymptotic results, together with the numerically optimized values, for transmission line parameters characteristic for one section per unit length. We can clearly see that the asymptotic formulas are accurate. It is quite impressive how well the asymptotic formula for intermediate T applies already to the case of one section per unit length.

Based on our analysis, we recommend as the definite criterion for choosing the optimal parameter value to compute for a given transmission line configuration and simulation time interval the three optimized parameters α_s^*, α_m^*, α_l^* according to the formulas (III.34,III.38,III.31), and then to choose the smallest one for the simulation, as indicated in Fig. 4.

IV. Numerical Experiments

We choose a 5 cm TEM mode transmission line model in Fig. 1 with 150 sections where the typical circuit parameters per unit length given in (III.29). Hence, for each section, we obtain the circuit elements

$$L_i = \frac{4.95e-3}{30}\ \mu\text{H},\ C_i = \frac{0.63}{30}\ \text{pF},\ R_i = \frac{0.5e-3}{30}\ \text{kOhms.}$$

For WR we chose one partition in the middle such that each end together with the connected circuitry can be analyzed separately. This prevents the formation of a large subsystem which may contain all the circuit connected to both ends of the TL. On purpose, we used a very asymmetrical reflective case with a source circuit with a $R_s = 0.05$ kOhms and a termination of $R_L = 0.0005$ kOhms. The source we use is $I_s = 20t$ mA for $0 < t < 0.1$ ns, and $I_s = 2$ mA for $t \geq 0.1$ ns, and the analysis time interval is $[0, T]$, where we will vary T to illustrate

T	classical	α_s^*	α_m^*	α_l^*
0.0025	3.52e-43	3.46e-43	2.77e-23	2.06e+00
0.025	8.88e-06	7.03e-06	1.08e-10	2.07e+00
0.25	4.01e-01	1.06e-06	2.87e-10	2.72e+00
2.5	2.10e+00	1.68e+00	2.84e-04	1.55e+00
25	1.94e+00	8.40e+01	2.47e-03	5.04e-01
250	1.89e+00	1.46e+02	2.95e-03	1.15e-02
2500	1.89e+00	1.88e+02	3.26e-03	2.50e-05
25000	1.89e+00	2.22e+02	3.37e-03	9.67e-11

TABLE I
COMPARISON OF THE ERROR LEVELS ACHIEVED BY THE CLASSICAL AND OPTIMIZED WAVEFORM RELAXATION ALGORITHMS AFTER 20 ITERATIONS, USING THE EXPLICIT ASYMPTOTICALLY OPTIMIZED FORMULAS FOR α_s^*, α_m^* AND α_l^*.

our theoretical results. We simply use 500 time steps, *i.e.* $\Delta t = T/500$ ns, and the backward Euler method to integrate in time. We show in Table I for various lengths of the time interval T, the error obtained after 20 iterations of the classical and optimized waveform relaxation algorithms, where error denotes the difference between the solution obtained by simulating the entire circuit, and the solution from the waveform relaxation algorithm. Table I illustrates the validity of our optimized parameter formulas. As expected, the asymptotic formula for short time achieves the best result for short time intervals T. Not surprising, it is close to the classical waveform relaxation algorithm. For large T, the asymptotic formula for long time gives the best result. As expected, the classical algorithm and the optimized one with the values suitable for short time are not converging. In between, over the large range from $T = 0.025$ to $T = 2500$ the intermediate formula gives by far the best results, while the other approaches showing severe convergence problems. In order to obtain a valid numerical comparison, we used in these experiments a highly oscillatory (random) initial waveforms. It is clear that for short time intervals, the signal does not reach the WR interface. Hence starting with a zero initial guess would lead to false convergence results.

We shown convergence results in Fig 5, for four different time intervals using now a zero initial waveform except for the shortest time example, for the same reason as in the previous paragraph. These results clearly confirm the importance of optimized waveform relaxation methods for the longitudinal partitioning of transmission line circuits.

We finally show in Fig. 6 the port voltages over time at the input and output of the transmission line for the case $T = 2.5$. The solid line in all the graphs shows the converged waveform for comparison. The dashed results in the figures on the left represent the results from a classical WR algorithm. We observe that convergence for the classical WR is extremely slow, as expected. The fast convergence is evident for the new optimized WR in the graphs on the right hand side. An accurate result is obtained in nine iterations without the subdivision of the

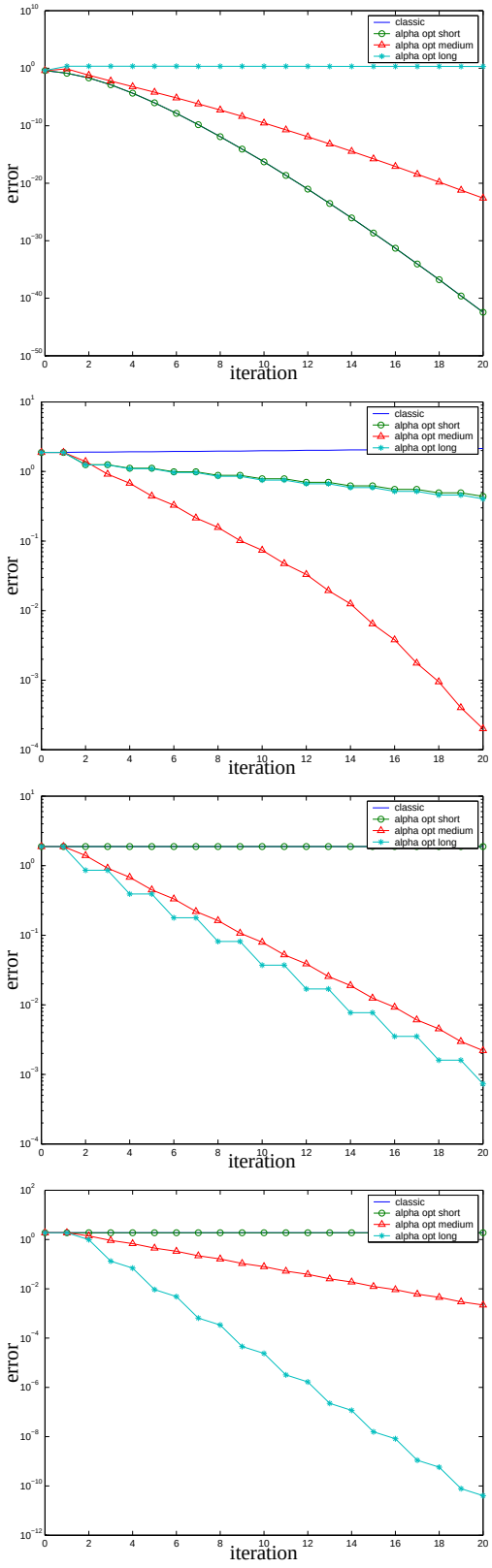

Fig. 5. Convergence behavior of the classical versus the optimized WR algorithms from top left to bottom right for $T = 0.0025$, $T = 2.5$, $T = 250$ and $T = 25000$, with a zero initial guess, except for the very short time interval, where a random initial guess was used, see text.

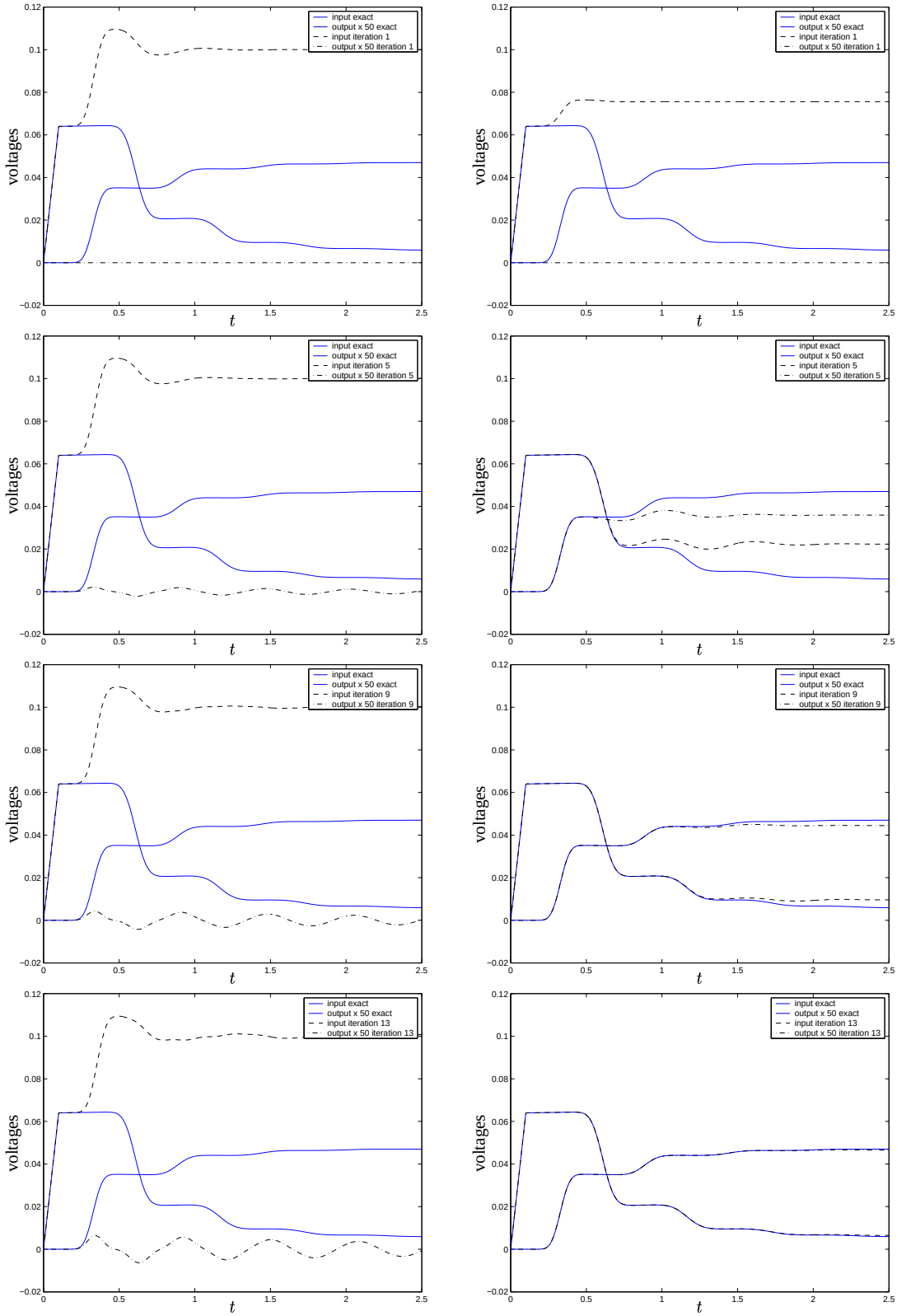

Fig. 6. Port voltages at the input and output of the transmission line, in solid the exact values, and in dashed on the left side iterates 1, 5, 9 and 13 for the classical WR, and on the right side in dashed the corresponding iterates for the new optimized WR.

time axis into time windows.

V. Conclusions

Prior to this work, we were unable to efficiently partition low loss transmission lines in the longitudinal direction using waveform relaxation. As is shown in this and other recent papers, the classical WR approach exhibits practical convergence problems for the longitudinal partitioning. Here we show that by using optimized transmission conditions, we can control the information exchange between subcircuits. This lead to explicit formulas for rapid convergence, using a new so called optimized waveform relaxation algorithm. Our numerical experiments confirm the good convergence results for longitudinal partitioning. This work also lays the foundation for the partitioning of other strongly coupled circuits.

This work, together with the recent work on classical transverse partitioning for multiconductor TL's leads to an efficient transient analysis approach for general multiconductor waveform relaxation since it was shown that the classical WR approach yields very good results for the transverse coupling for multiple lines.

References

[1] Q. Yu, J. M. L. Wang, and E. Kuh, "Passive multipoint moment matching model order reduction algorithm on multiport distributed interconnect networks," *IEEE Transactions on Circuits and Systems, I*, pp. 140–160, Jan. 1999.

[2] T. Kim, X. Li, and D. J. Allstot, "Compact model generation for on-chip transmission lines," *IEEE Transactions on Circuits and Systems, I*, pp. 459–470, Mar. 2004.

[3] F. H. Branin, "Transient analysis of lossless transmission lines," *Proceedings of the IEEE*, vol. 55, pp. 2012–2013, Nov. 1967.

[4] C. Paul, *Analyis of multiconductor transmission lines*. John Wiley, 1992.

[5] G. Antonini and G. Ferri, "A new approach for closed form transient analysis for multiconductor transmission lines," *IEEE Transactions on Electromagnetic Compatibility*, vol. 46, pp. 529–543, Nov 2004.

[6] E. Gad, C. Chen, and M. Nakhla, "Passivity verifi cation in delay-based macromodels of electrical interconnects," *IEEE Transactions on Circuits and Systems, I*, pp. 2173–2187, Oct. 2005.

[7] A. J. Gruodis and F. Y. Chang, "Coupled lossy transmission line characterization and simulation," *IBM Journal of Research and Development*, vol. 25, pp. 25–41, Jan. 1981.

[8] S. Grivet-Talocia, H.-M. Huang, A. Ruehli, F. Canavero, and I. Elfadel, "Transient analysis of lossy transmission line: An effi cient approach based on the method of characteristics," *IEEE Transactions on Advanced Packaging*, vol. 27, pp. 45–56, Feb. 2004.

[9] N. Nakhla, A. Ruehli, M. Nakhla, R. Achar, and C. Chen, "Waveform relaxation techniques for simulation of coupled interconnects with frequency-dependent parameters," *IEEE Transactions on Advanced Packaging*, vol. 30, no. 2, pp. 257–269, May 2007.

[10] G. Antonini, "A dyadic Green's function based method for the transient analysis of lossy and dispersive multiconductor transmission lines," *IEEE Transactions on Microwave Theory and Techniques*, vol. 56, pp. 880–895, Apr. 2008.

[11] E. Lelarasmee, A. E. Ruehli and A. L. Sangiovanni-Vincentelli, "Waveform relaxation decoupling method," *IBM Tech. Disclosure Bulletin*, vol. 24, no. 7B, p. 3720, Dec. 1981.

[12] ——, "The waveform relaxation method for time-domain analysis of large-scale integrated circuits," *IEEE Trans. on CAD of Integrated Circuits and Systems*, vol. CAD-1(3), pp. 131–145, July 1982.

[13] F. Y. Chang, "The generalized method of characteristics for waveform relaxation analysis of lossy coupled transmission lines," *IEEE Transactions on Microwave Theory and Techniques*, vol. 37, pp. 2028–2038, Dec. 1989.

[14] J. K. White A. Sangiovanni-Vincentelli, *Relaxatioon Techniques for the Simulation of VLSI Circuits*. Kluwer Academic Publishes, Boston, 1986.

[15] A. E. Ruehli, Ed., *Circuit Analysis, Simulation and Design*. Elseviers, North-Holland, New York, Amsterdam, 1987.

[16] A. E. Ruehli and T. A. Johnson, *Circuit Analysis Computing by Waveform Relaxation*. New York: Wiley Encyclopedia of Electrical Electronics Engineering, 1999, vol. 3.

[17] J. White, and A. L. Sangiovanni-Vincentelli, "Partitioning algorithms and parallel implementations of waveform relaxation algorithms for circuit simulation," in *IEEE Proc. Int. Symp. on Circuits and Systems (ISCAS)*, June 1985, pp. 1069–1072.

[18] M. J. Gander and A. Stuart, "Space-time continuous analysis of waveform relaxation for the heat equation," *SIAM Journal on Scientific Computing*, vol. 19, no. 6, pp. 2014–2031, 1998.

[19] E. Giladi and H. B. Keller, "Space time domain decomposition for parabolic problems," *Numerische Mathematik*, vol. 93, no. 2, pp. 279–313, 2002.

[20] M. J. Gander, L. Halpern, and F. Nataf, "Optimal convergence for overlapping and non-overlapping Schwarz waveform relaxation for time dependent problems," in *Proceedings of the Eleventh International Conference on Domain Decomposition Methods*, C.-H. Lai, P. Bjørstad, M. Cross, and O. Widlund, Eds. ddm.org, 1998, held in Greenwich, Great Britain, July 20-24, 1998.

[21] M. J. Gander and L. Halpern, "Méthodes de relaxation d'ondes pour l'équation de la chaleur en dimension 1," *C.R. Acad. Sci. Paris, Série I*, vol. 336, no. 6, pp. 519–524, 2003.

[22] M. J. Gander, L. Halpern, and F. Nataf, "Optimal Schwarz waveform relaxation for the one dimensional wave equation," *SIAM Journal of Numerical Analysis*, vol. 41, no. 5, pp. 1643–1681, 2003.

[23] M. J. Gander and L. Halpern, "Optimized Schwarz waveform relaxation methods for advection reaction diffusion problems," *SIAM J. Numer. Anal.*, vol. 45, no. 2, pp. 666–697, 2007.

[24] V. B. Dmitriev-Zdorov and B. Klaassen, "An improved relaxation approach for mixed system analysis with several simulation tools," in *Proc. of EURO-DAC'95, IEEE Comp. Soc. Press*, 1995.

[25] V. B. Dmitriev-Zdorov, "Generalized coupling as a way to improve the convergence in relaxation-based solvers," in *Design Automation Conference, 1996, with EURO-VHDL '96 and Exhibition, Proceedings EURO-DAC '96, European*, 1996, held in Geneva, Switzerland, Sept. 1996.

[26] M. J. Gander and A. Ruehli, "Optimized waveform relaxation methods for RC type circuits," IBM Research Report, NY 10598, Tech. Rep. RC22207, October 2001.

[27] M. J. Gander and A. E. Ruehli, "Solution of large transmission line type problems using a new optimized waveforms relaxation partitioning," in *Proc. IEEE International Conference on EMC*, Boston,MA, Aug. 2003.

[28] M. J. Gander, M. Al-Khaleel, and A. E. Ruehli, "Waveform relaxation technique for longitudinal partitioning of transmission lines," in *Digest of Electr. Perf. Electronic Packaging*, 2006, pp. 207–210.

[29] M. Al-Khaleel, "Optimized waveform relaxation methods for circuit simulations," Ph.D. dissertation, McGill University, 2007.

[30] B. Leimkuhler, A. Ruehli, "Rapid convergence of waveform relaxation," *Appl. Numer. Mathematics.*, vol. 11, pp. 211–224, July 1993.